Eur. Phys. J. B **12**, 91–97 (1999)

THE EUROPEAN PHYSICAL JOURNAL B

EDP Sciences

Structure and size distribution of percolating clusters. Comparison with gelling systems

J.C. Gimel[1,a], T. Nicolai[1], D. Durand[1,b], and J.M. Teuler[2]

[1] Chimie et Physique des Matériaux Polymères[c], Université du Maine, 72085 Le Mans Cedex 9, France
[2] IDRIS, Bâtiment 506, B.P. 167, 91403 Orsay Cedex, France

Received 16 December 1998 and Received in final form 21 April 1999

Abstract. 3d lattice Monte-Carlo simulations were done to obtain the mass distribution ($N(m)$) and pair correlation function ($g(r)$) of percolating clusters. We give analytical expressions of the external cut-off functions of $N(m)$ at the z-average mass and of $g(r)$ at the radius of gyration. The simulation results were compared with experimental results on gel forming systems reported in the literature. The comparison shows that the experimental results are compatible with the simulation results. However, more experiments are needed before we can be confident that the percolation model is a good model for the sol-gel transition.

PACS. 82.70.Gg Gels and sols – 83.80.Jx Chemically reactive materials – 64.60.Ak Renormalization-group, fractal, and percolation studies of phase transitions – 02.70.Lq Monte-Carlo and statistical methods

1 Introduction

Two decades ago it was suggested [1] that the gelation process close to the gel point can be described by the percolation model. There exists no analytical theory for percolation in 3 dimensions, but it can be simulated numerically. Percolating clusters have the following characteristics [2]:

$$\begin{array}{lll} N(m) & \propto m^{-\tau} f(m/m_z) & m \gg 1 \text{ and } m_z \gg 1 \\ m & \propto R_{\mathrm{g}}^{d_f} & m \gg 1 \\ g(r) & \propto r^{d_f-3} h(r/R_{\mathrm{g}}) & r \gg r_0 \text{ and } R_{\mathrm{g}} \gg r_0 \\ m_z & \propto \varepsilon^{-1/\sigma} & \varepsilon \to 0 \end{array} \quad (1)$$

Here $N(m)$ is the number of clusters per unit volume with aggregation number m and radius of gyration R_{g} and $g(r)$ is the pair correlation function. $f(x)$ and $h(x)$ are cut-off functions at the z-average aggregation number, m_z, and the radius of gyration (R_{g}), which are unity for $x \ll 1$ and decrease faster than any power law for $x \gg 1$. d_f is the so-called fractal dimension and r_0 is the size of the elementary unit of the clusters. ε is a parameter which characterizes the distance to the gel point: $\varepsilon = |p - p_{\mathrm{c}}|/p_{\mathrm{c}}$, where p is the extent of connectivity and p_{c} is the value at the gel point. Other properties of percolating clusters are easily derived from equation (1), *e.g.* the divergence of the weight average aggregation number (m_w) or the relation between m_w and the z-average radius of gyration ($R_{\mathrm{g}z}$): $m_w \propto \varepsilon^{-(3-\tau)/\sigma}$, $m_w \propto R_{\mathrm{g}z}^{d_f(3-\tau)}$. Computer simulations have been used to obtain the values of the exponents: $\tau = 2.19$, $d_f = 2.53$ and $\sigma = 0.45$ [3].

The static properties of percolating clusters form the basis of attempts to explain the effects of gel formation on the mechanical properties, such as the dependence of the viscosity and the gel modulus on ε and the low frequency dependence of the shear modulus close to the gel point [4]. Of course, assumptions in addition to percolation have to be made to explain dynamic properties. In order to test the validity of these additional assumptions we have to make sure that the static properties of real clusters close to the gel point are indeed those of percolating clusters obtained from computer simulations.

Experimental studies have been done in order to see if the characteristics of the clusters close to the gel point correspond to those of percolating clusters. These experiments were almost exclusively aimed at obtaining values of the exponents. The exponent τ can in principle be determined using size exclusion chromatography (SEC) in combination with light scattering detection. Of course, the correct value of τ is only obtained in the size range $r_0 \ll R_{\mathrm{g}} \ll R^*$ where R^* is either $R_{\mathrm{g}z}$ or the upper limit of the resolution of the SEC columns used. The upper limit of resolution of the commercially available columns is about 70 nm while r_0 is generally at least a few nanometers. A number of gel forming systems have been investigated with SEC and give $\tau \approx 2.2$ [5–8].

The structure of percolating clusters can be studied using scattering methods. The scattering wave vector (q) dependent structure factor $S(q)$ is the Fourier transform of $g(r)$ [9]. Direct experimental determination of d_f is extremely difficult. Real clusters are flexible

[a] e-mail: Jean-Christophe.Gimel@univ-lemans.fr
[b] e-mail: Dominique.Durand@univ-lemans.fr
[c] UMR6515 CNRS

and their fractal dimension decreases upon dilution. In addition, the measured fractal dimension (d_f^*) of the whole system is modified by the effect of polydispersity: $d_f^* = d_f(3-\tau)$ [10]. Direct determination of d_f is only possible by measuring the scattering intensity of a monodisperse labelled fraction of the clusters in the bulk [11]. This experiment has not been attempted. Adam *et al.* [12] have measured the structure factor of one polydisperse bulk system using neutron scattering. They found $d_f^* = 2.0$ and using an independent measure of $\tau = 2.2$ obtained $d_f = 2.5$. All other measurements, see *e.g.* [10,13,14], have been done on clusters swollen in a good solvent. The fractal dimension of swollen clusters, d_{fs}, is not directly related to d_f, but can be related to the spectral dimension which takes into account the connectivity of the clusters [15] which leads to $d_{fs} = 2$.

Experimental determination of σ requires the measurement of m_z as a function of p close to p_c. In practice one assumes that p is proportional to measurable parameters such as the reaction extent or the amount of added cross-linking agent at complete reaction. Most often m_w is determined using scattering techniques, so one needs an independent measure of τ to determine σ. The limitation of such measurements is the accuracy with which p_c and p can be determined. Experimental results on a number of systems are in agreement with simulation results of percolating clusters even though in most cases rather large values of ε where used [6,16–19].

In all experiments it was assumed that the influence of internal and external cut-off functions of the power law behaviour was negligible for the range of data used to obtain the exponents. Since the cut-off functions are very smooth the extent of their influence cannot be detected in the data that contain noise, but has to be assumed negligible. However, in [20] we have shown that the influence of internal and external cut-off functions can be quite strong.

It is important to know the form of the cut-off functions in order to estimate whether they can be neglected. In computer simulations internal cut-off functions and thus the prefactors in equation (1) depend on the way percolation is modelled. For real systems they depend on the structure of the precursors. Unfortunately, care has not always been taken to ensure that experimental values of m or q^{-1} are sufficiently large compared to the elementary unit. In addition, if percolation is a good model for gelation then the external cut-off functions should be system independent [2] and the same as in computer simulations. Knowledge of these cut-off functions not only allows one to estimate their influence on the data, but could also be used directly in the analysis. Stauffer [21] showed a rough estimate of $f(m/m_z)$ obtained from Monte-Carlo simulations, but did not give an analytical expression. As far as we are aware the structure factor of individual percolating clusters has not been calculated and $g(r/R_g)$ is unknown.

Here we present Monte-Carlo simulations of site percolation on cubic lattices. We focus on the results extrapolated to infinite lattice size. A detailed discussion of finite size effects will be given elsewhere. Finite size effects are important in computer simulations, but not relevant for comparison with real systems. We will compare $N(m)$ and $S(q)$ obtained from computer simulations with literature results for real systems.

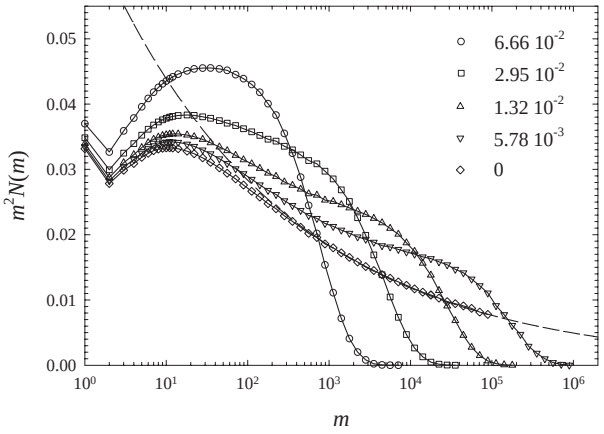

Fig. 1. $m^2N(m)$ at different values of ε as indicated in the figure obtained by extrapolation to $L \to \infty$. The dashed line represents the power law asymptotic behaviour at $\varepsilon = 0$.

2 Results

2.1 Mass distribution

We have used two methods to simulate percolating clusters. In the first one sites on cubic lattices with size L^3 were occupied with probability ϕ. Neighbouring sites were taken as connected. The number of clusters with m sites ($N(m)$) was determined at different values of L and ϕ. The results were averaged over a large number of trials in order to reduce the standard error to less than 1%. We define that the system percolates if at least one cluster spans the lattice in at least one direction. The critical density, ϕ_c, for percolation for $L \to \infty$ was found to be 0.3116 in good agreement with literature results. ε is calculated as $\varepsilon = |\phi_c - \phi|/\phi_c$. Extrapolations to $L \to \infty$ at different values of ε were done by plotting the data as a function of $1/L$. For small m, $N(m)$ increases linearly with $1/L$ up to the smallest L used. The linear range decreases with increasing m and the largest value of m for which $N(m)$ can be determined accurately depends on L. Using lattices with L up to 1023, the smallest ε for which $N(m)$ can be determined accurately over the whole range of m is about 6×10^{-3}.

In the second so-called Leath method [22] sites adjacent to a seed site are occupied with probability ϕ. In subsequent steps non-tested sites adjacent to filled sites are occupied with probability ϕ. With this method finite size effects can be avoided by choosing the seed in the center of the box and keeping the maximum cluster size below that of the lattice. This method has about the same limitations as the previous method and gives the same results.

Figure 1 shows $N(m)$ extrapolated to $L \to \infty$ at different values of ε below the percolation threshold. We have

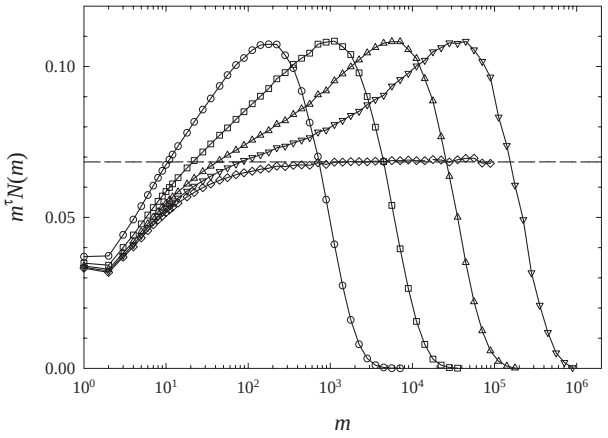

Fig. 2. $m^\tau N(m)$ at different values of ε as indicated in Figure 1 obtained by extrapolation to $L \to \infty$ with $\tau = 2.19$.

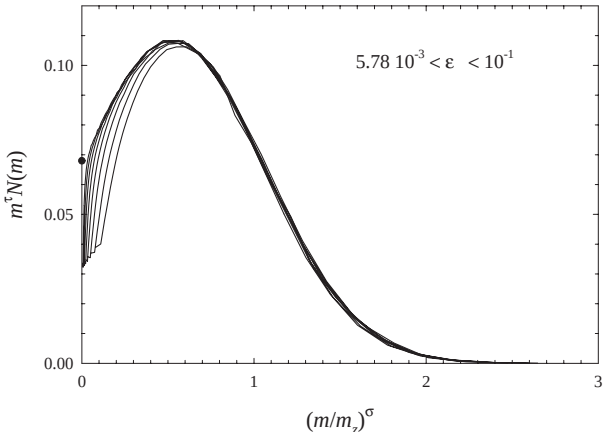

Fig. 3. Same data as in Figure 2 plotted as a function $(m/m_z)^\sigma$ with $\sigma = 0.45$. The filled circle represents the power law asymptotic behaviour at $\varepsilon = 0$.

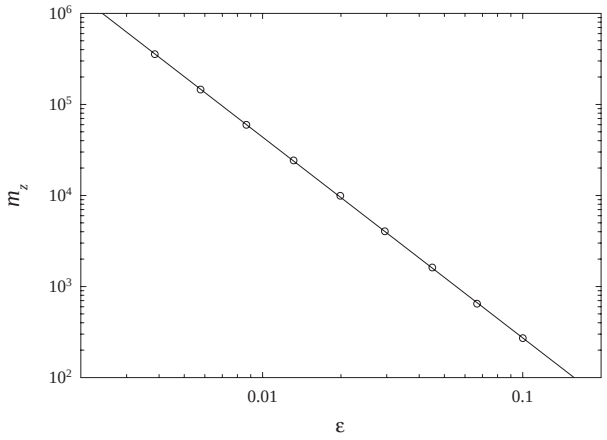

Fig. 4. Dependence of m_z on ε. The solid line represents the result of a linear least squares fit to the data: $m_z = 1.65 \times 10^{-2.21}$

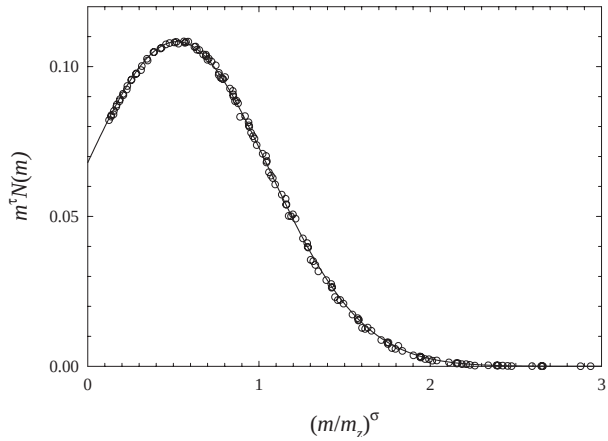

Fig. 5. External cut-off function of the mass distribution of percolating clusters obtained from 3d Monte-Carlo simulations. The solid line represents the result of a non-linear least squares fit given by equation (2).

plotted $m^2N(m)$ to facilitate comparison with SEC results, see Section 3.1. On the other hand, the effect of internal and external cut-off functions is best visualized by plotting $m^\tau N(m)$ which is constant if the effect is absent. If the correct value of τ is used the amplitude of $m^\tau N(m)$ should be independent of ε for $\varepsilon \ll 1$. This is the case for $\tau = 2.19$, see Figure 2, which agrees with the literature value. Note that there is no range of m over which the effect of both the internal and external cut-off can be neglected even at the smallest ε used in the simulations. In Figure 3 we have plotted $m^\tau N(m)$ as a function of $(m/m_z)^\sigma$. In this representation the data should collapse on a single curve which represents $f(m/m_z)$. Deviations at small values of m/m_z are due to the internal cut-off and are more important for larger $\varepsilon \cdot m_z$ scales with ε over the whole range tested: $m_z = 1.70\varepsilon^{-2.21}$, see Figure 4. This means that $\sigma = 0.45$, in agreement with values given in the literature.

Stauffer [21] suggested that $f(m/m_z)$ can be described by a Gaussian function in terms of $(m/m_z)^\sigma$. Figure 5 shows that a Gaussian gives indeed a very good description of $f(m/m_z)$ at least for $\phi < \phi_c$. In Figure 5 we used $\sigma = 0.45$ and have retained the data shown in Figure 3 that are not influenced by the internal cut-off. A non-linear least squares fit gives:

$$m^\tau N(m) = 0.108 \exp\left[-\left(\frac{(m/m_z)^\sigma - 0.521}{0.763}\right)^2\right]. \quad (2)$$

Note that we have obtained the cut-off function by extrapolating to $L \to \infty$ contrary to Stauffer [21] who used $f(x) = N(m,\varepsilon)/N(m,\varepsilon = 0)$ for a given lattice size. This procedure assumes that finite size effect can be simply divided out. Elsewhere we will show that this assumption is not justified and leads to erroneous results. We will also show there that the Gaussian form is only a rough approximation for the cut-off function for $\phi > \phi_c$.

2.2 Structure

Percolating clusters with a given mass have a range of structures. Each structure can be characterized by a radius

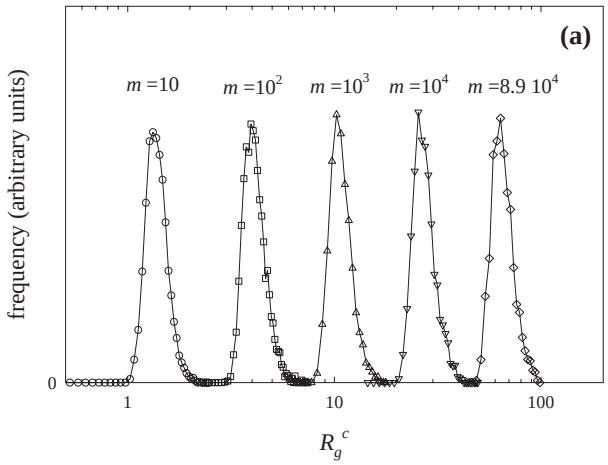

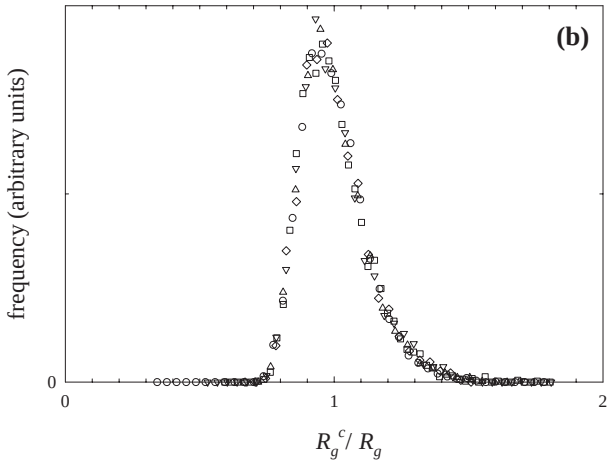

Fig. 6. (a) Histogram of $R_{\rm g}^{\rm c}$ on a logarithmic scale for simulated percolating clusters with different aggregation numbers indicated in the figure. (b) Same data as a function of $R_{\rm g}^{\rm c}/R_{\rm g}$.

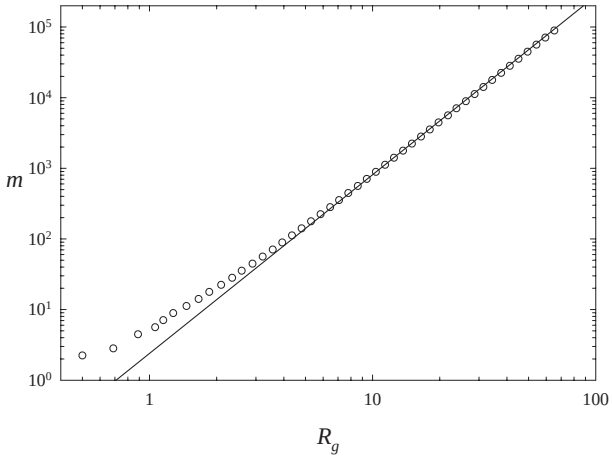

Fig. 7. Evolution of the aggregation number with the radius of gyration of simulated percolating clusters.

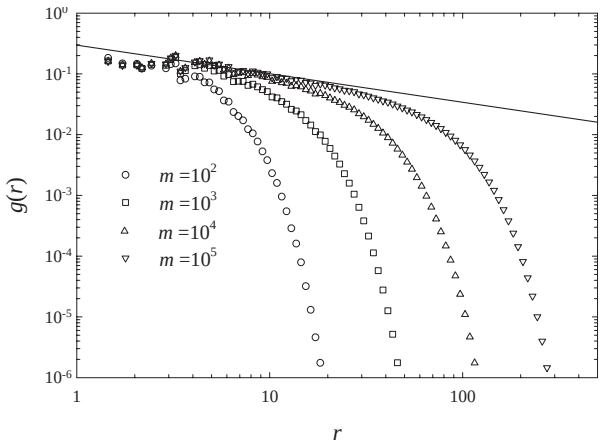

Fig. 8. Average pair correlation function of simulated percolating clusters with different aggregation numbers indicated in the figure.

of gyration, $R_{\rm g}^{\rm c}$. The superscript c is used to distinguish this radius of gyration from the average radius of gyration for a given mass. The distribution of structures for a given value of m can thus be characterized by the distribution of $R_{\rm g}^{\rm c}$. In Figure 6a we have plotted the distribution of $R_{\rm g}^{\rm c}$ at different m. Figure 6b shows that the relative width of this distribution is independent of m. For flexible clusters the radius of gyration will vary in time and the time averaged value will be very close to the structure averaged value $R_{\rm g}$. We show in Figure 7 the evolution of $R_{\rm g}$ with m for $R_{\rm g}$ much smaller than L so that finite size effects can be neglected. A linear least squares fit for $m > 10^4$ gives $m = 2.4R_{\rm g}^{2.53}$ which is in agreement with the values of d_f reported in the literature.

The average pair correlation function ($g(r)$) of percolating clusters with different m is shown in Figure 8. For clusters with $m \leq 10^4$, $g(r)$ has been calculated by computing the $m(m-1)/2$ pair distances in the cluster. For bigger clusters, we have sampled at least 10^8 pairs in the cluster. The average has been taken over at least 100 clusters of mass m. $g(r)$ has been normalized so that $\int 4\pi r^2 g(r) {\rm d}r = m$. For large m we observe a power law dependence of $g(r)$ in agreement with equation (1). The scatter in the data at small r reflects the discrete nature of the lattice. The shape of the external cut-off is independent of m and is well described by a stretched exponential, see Figures 9a and 9b:

$$r^{3-d_f} g(r) = 0.29 \exp\left[-\left(\frac{r}{1.1R_{\rm g}}\right)^{1.7}\right]. \qquad (3)$$

In the fit we have used the relation between m and $R_{\rm g}$ to reduced the number of free parameters from 3 to 1 see [9] for details.

3 Discussion

3.1 Mass distribution

In SEC the cluster weight concentration ($C \propto mN(m)$) is measured as a function of the elution volume ($V_{\rm e}$). SEC

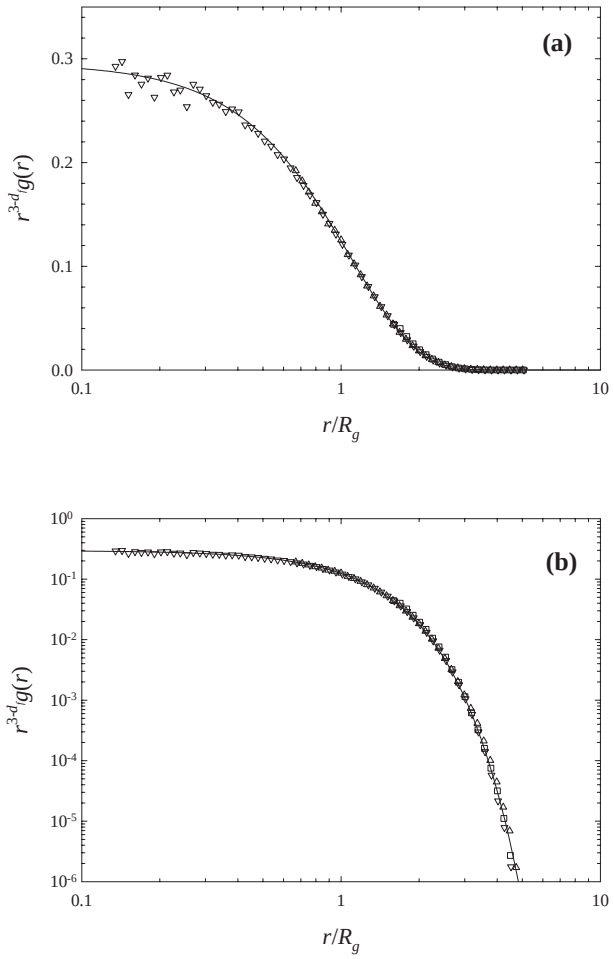

Fig. 9. (a) $r^{3-d_f}\,g(r)$ as a function of (r/R_g) with $d_f = 2.53$ for percolating clusters obtained from 3d Monte-Carlo simulations. Same symbols as in Figure 8. The solid line represents the fit given by equation (3).(b) Double logarithmic representation of the same data.

columns exist for which $V_\mathrm{e} \propto \log m$ over a broad range of m. In this case experimental chromatograms of systems close to the gel point can be directly compared to Figure 1 as long as the largest clusters are not totally excluded. If the SEC columns are not linear, a calibration curve should be employed or the molar mass should be determined using on-line light scattering detection.

As in the computer simulations, chromatograms of real systems show the influence of internal and external cut-offs of the power law dependence. In the simulations the effect of the internal cut-off becomes negligible only for $m > 200$. However, as mentioned above the internal cut-off depends on the type of simulation and is system dependent for real systems. On the other hand, for percolating clusters, the external cut-off is system independent and given by equation (2).

Experimentally, τ is determined by measuring the slope of $\log C$ *versus* $\log m$. The external cut-off modifies this slope close to m/m_z. Of course, the influence of the external cut-off can be avoided by taking systems with very large m_z. However, in this case the cut-off in the chromatogram at large m depends on the resolution of the column used. Total exclusion leads to a peak in the chromatogram at a high molar mass. It is unknown up to what value of m the effect of the column resolution can be neglected. A direct comparison of experimental chromatograms with equation (2) represents a more stringent test of the applicability of the percolation to the gelation of real systems. In SEC combined with on-line light scattering detection one obtains $m^3N(m)$ as a function of $\log m$. In this representation the SEC signal has a maximum at m_max. It is straightforward to calculate that if the external cut-off function is given by equation (2) then $m_\mathrm{max} = 0.79m_z$, independent of the internal cut-off function.

A number of gel forming systems have been investigated using SEC [5–8]. In all cases values of τ close to 2.2 have been reported. In two cases an attempt was made to determine $f(m/m_z)$ [5,8]. In [6] a simple exponential cut-off was assumed. Unfortunately, these SEC results are not sufficiently precise to distinguish between an exponential and a Gaussian cut-off function.

Dynamic light scattering (DLS) is an alternative way to measure the molar mass distribution of the clusters. In DLS the intensity auto correlation function (g_2) is measured which can be related to the electric field autocorrelation function (g_1) [23]. For solutions g_1 is given by the inverse Laplace transform of the relaxation time distribution of concentration fluctuations ($A(\tau_r)$): $g_1(t) = \int_0^\infty A(\tau_r)\exp(-t/\tau_r)\,\mathrm{d}\tau_r$. In the case of very dilute solutions and at $qR_{\mathrm{g}z} < 1$ concentration fluctuations occur *via* translational diffusion. In this case τ_r is related to the diffusion coefficient: $\tau_r = 1/(q^2D)$. The diffusion coefficient is inversely proportional to the hydrodynamic radius (R_h). For highly diluted large percolating clusters it is reasonable to assume no draining so that $m \propto R_\mathrm{h}^{d_f}$. The relaxation time is thus related to the mass: $\tau_r = am^{1/d_f}$ with a a constant. This means that for $m \gg 1$ and $qR_{\mathrm{g}z} < 1$:

$$g_1(t) \propto \int_1^\infty m^3N(m)\exp\left(-\frac{t}{am^{1/d_f}}\right)\mathrm{d}\log m. \qquad (4)$$

The upper limit of m that can be determined by DLS is given by the condition $qR_{\mathrm{g}z} < 1$. In practice the limiting size is about 300 nm, *i.e.* much higher than in SEC. Unfortunately, a direct inverse Laplace transformation of g_1 is very sensitive to noise, which means that $N(m)$ cannot be obtained from g_1 without some ambiguity. Nevertheless, DLS offers an opportunity to test whether a particular form of $N(m)$ agrees with the data. In Figure 10 we show correlograms obtained from dilute solutions of cross-linked PMMA at different reaction extents close to the gel point. Care was taken to ensure that $qR_{\mathrm{g}z} < 1$. The time axis is normalized by the average relaxation rate, $\langle\Gamma\rangle = \langle\tau_r^{-1}\rangle$, which leads to superposition over the whole time range demonstrating that the mass distribution and the structure does not vary with the reaction extent. The correlograms are compared to equation (4) using the fractal dimension of swollen clusters, $d_{f\mathrm{s}} = 2$, and either equation (2) or a simple exponential for the cut-off function.

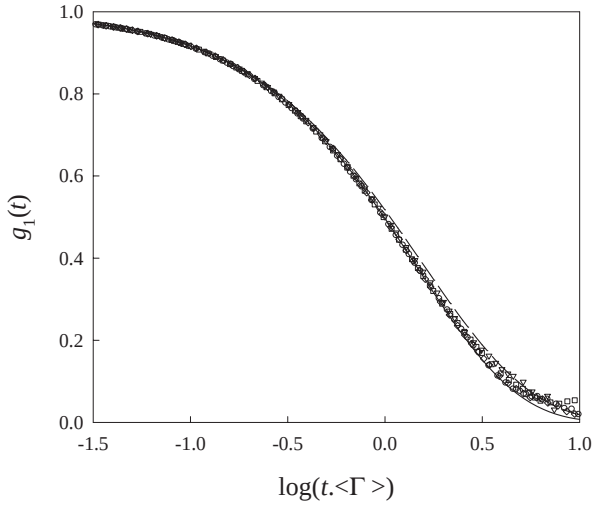

Fig. 10. Electric field autocorrelation functions of diluted solutions of cross-linked PMMA at different reaction extents close to the gel point. Care was taken to ensure that $qR_{gz} < 1$. The time axis is normalized by the average relaxation rate. The solid line represents the result of a non-linear least squares fit to equation (4) with $d_f = 2$ and $N(m)$ given by equation (1) using $\tau = 2.19$ and $f(m/m_z)$ given by equation (2). The dashed line represents a fit with a exponential cut-off function for $f(m/m_z)$.

g_1 is very sensitive to trace amounts of spurious scatterers which give rise to a small baseline. Nevertheless, it is clear that equation (2) gives a better description of the data than a simple exponential cut-off. The effect of different cut-off functions becomes negligible for $t.\langle\Gamma\rangle < 0.5$. For more details of the properties of this system see [24].

3.2 Structure

As mentioned in the introduction, as far as we are aware, only one experimental structure factor has been reported of an undiluted polydisperse system (polyurethane) close to the gel point [12]. The structure factor was measured for a mixture of hydrogenated and deuterated polyurethane using SANS. Under the assumption of no specific interaction between hydrogenated and deuterated polyurethane, the labelling technique ensures that interparticle interactions do not contribute to the structure factor [25]. We have calculated $S(q)$ of percolating clusters by taking the Fourier transform of $g(r)$. The z-average structure factor of the polydisperse system was calculated as:

$$S_z(q) = \frac{\int_1^\infty m^2 N(m) S(q)\,\mathrm{d}m}{\int_1^\infty m^2 N(m)\,\mathrm{d}m} \qquad (5)$$

using the Gaussian cut-off function of $N(m)$ given in equation (2).

Figure 11 shows the experimental results together with $S_z(q)$ using for $h(r/R_g)$ a simple exponential or the stretched exponential given in equation (3). It is clear that the stretched exponential gives a better description

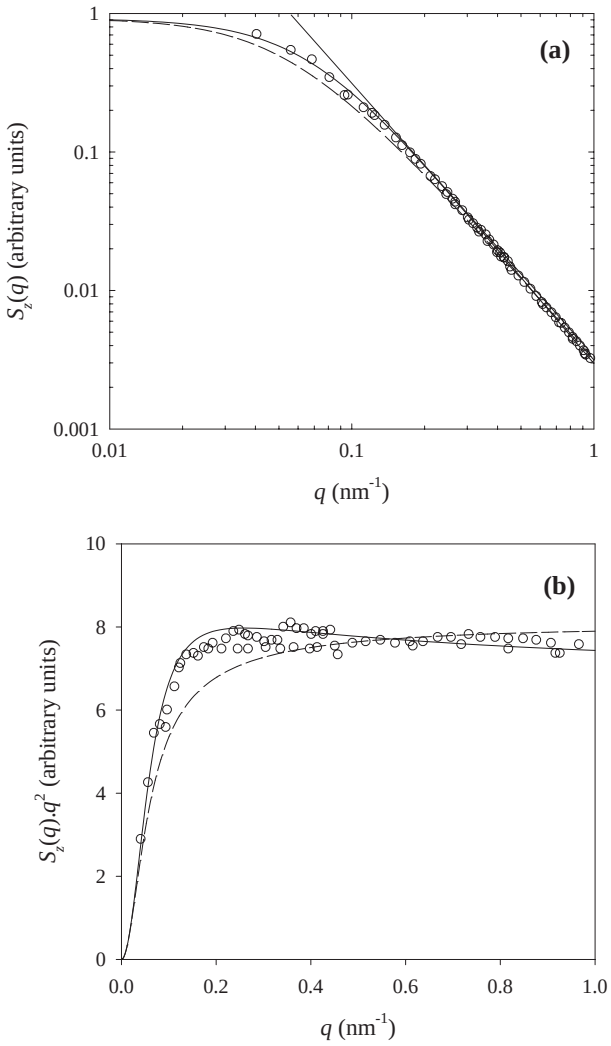

Fig. 11. (a)Comparison of the experimental structure factor of polydisperse branched polyurethane close to the gel point and the z-average structure factor of simulated percolating clusters using for $h(r/R_g)$ a stretched exponential cut-off (solid line) and a simple exponential cut-off (dashed line). The straight line has a slope of 2. (b) Different representation of the same data.

of the data. Unfortunately, at larger q-values the condition $qr_0 \ll 1$ is no longer valid and the internal cut-off cannot be neglected. It is difficult to estimate precisely the size below which the polyurethane clusters no longer have the self similar structure of the branched clusters. It is, of course, bigger that the size of the prepolymers used to make the clusters which is a few nanometers. The crossover to the local structure cannot be seen in the experiment because the fractal dimension of the first few oligomers which are essentially linear is 2, *i.e.* very close to that of polydisperse percolating clusters ($d_f^* = d_f(3-\tau)$). The q-range over which both the internal and the external cut-off functions can be neglected is very small indeed. It is clearly not justified to deduce the fractal dimension of the clusters from the data without knowledge of the effect of the cut-off functions. The present analysis gives

more confidence that the large scale structure of the polyurethane clusters is indeed the same as that of the percolating clusters obtained from computer simulations.

A lot of experimental work is done on diluted systems. We are currently attempting to simulate the effect of swelling in order to obtain the structure factor of percolating clusters swollen in good solvents.

4 summary

We have simulated the structure and mass distribution of percolating clusters including the external cut-off functions. We have compared the simulation results with experimental results on gelling systems. The mass distribution of a number of systems is in agreement with simulation results, although only for one system can the simulated and experimental external cut-off function be compared quantitatively. Only one experimental structure factor of an undiluted gel forming system has been reported. This experimental result is compatible with simulation results, but the average cluster size was small so that the effect of the internal cut-off function is important in the experiment. It is clear that more measurements are needed on large clusters of various gelling systems, before one can conclude with confidence that the percolation model describes the sol-gel transition for real systems.

References

1. P.G. de Gennes, *Scaling concepts in polymer physics* (Cornell University Press, Ithaca, 1979).
2. D. Stauffer, A. Aharony, *Introduction to percolation theory*, 2nd edn. (Taylor & Francis, London, 1992).
3. R. Ziff, G. Stell, Laboratory for Scientific Computing of College of Engineering, Report No. 88-4, University of Michigan, 1988 (unpublished); P. Grassberger, J. Phys. A **25**, 5867 (1992); N. Jan, D. Stauffer, Int. J. Mod. Phys. C **9**, 341 (1998).
4. J.E. Martin, A. Adolf, Annu. Rev. Phys. Chem. **42**, 311 (1991); M. Rubinstein, R.H. Colby, J.R. Gillmo, in *Space-Time Organisation in Macromolecular Fluids*, edited by F. Tanaka, M. Doi, T. Ohta (Springer, Berlin, 1989).
5. F. Schosseler, H. Benoit, Z. Gubisic-Gallot, C. Strazielle, L. Leibler, Macromolecules **22**, 400 (1989).
6. E.V. Patton, J.A. Wesson, J.C. Rubinstein, J.C. Wilson, L.E. Oppenheimer, Macromolecules **22**, 1946 (1989).
7. J. Bauer, W. Burchard, Macromolecules **26**, 3103 (1995).
8. C. Degoulet, T. Nicolai, D. Durand, J.P. Busnel, Macromolecules **28**, 6819 (1995).
9. T. Nicolai, D. Durand, J.C. Gimel, in *Light Scattering: Principles and Development*, edited by W. Brown (Clarendon Press, Oxford, 1996).
10. J.E. Martin, B.J. Ackerson, Phys. Rev. A **31**, 1180 (1985).
11. M. Daoud, Prog. React. Kinet. **15**, 1 (1989).
12. M. Adam, D. Lairez, F. Boué, J.P. Busnel, D. Durand, T. Nicolai, Phys. Rev. Lett. **67**, 3456 (1991).
13. J.E. Martin, K.D. Keefer, Phys Rev. A **34**, 4988 (1986).
14. E. Bouchaud, M. Delsanti, M. Adam, M. Daoud, D. Durand, J. Phys. France **47**, 1273 (1986).
15. M.E. Cates, J. Phys. Lett. France **46**, 757 (1985).
16. S.J. Candau, M. Ankrim, J.P. Munch, in *Physical Optics of Dynamic Phenomena and Processes in Macromolecular Systems*, edited by B. Sedlacek (Walter de Gruyter, Berlin, 1985).
17. C. Collette, F. Lafuma, R. Audebert, L. Leibler, in *Biological and Synthetic Networks*, edited by O. Kramer (Elsevier, Amsterdam, 1988).
18. D. Adolf, J.E. Martin, Macromolecules **23**, 3700 (1990).
19. D. Durand, M. Adam, M. Delsanti, J.P. Munch, in *Universalities in Condensed Matter Physics*, edited by R. Jullien, L. Peliti, R. Ramal, N. Boccara, *Proceedings in Physics* (Springer, Berlin, 1988), Vol. 32.
20. T. Nicolai, D. Durand, J.C. Gimel, Phys. Rev. B **50**, 16357 (1994).
21. D. Stauffer, in *On Growth and Form. Fractal to Non-Fractal Patterns in Physics*, edited by H.E. Stanley, N. Ostrowski (Martin Nijhoff Publishers, Boston, 1986).
22. P.L. Leath, Phys. Rev. B **14**, 5046 (1976).
23. B. Berne, R. Pecora, *Dynamic Light Scattering* (Wiley, New York, 1976).
24. V. Lesturgeon, T. Nicolai, D. Durand, Eur. Phys. J. B **9**, 83 (1999).
25. see for example D.G. Wignall, in *Physical properties of polymers*, 2nd edn. (American Chemical Society, Washington DC, 1993), Chap. 7.